© 2018. Published by The Company of Biologists Ltd | Journal of Experimental Biology (2018) 221, jeb184713. doi:10.1242/jeb.184713

RESEARCH ARTICLE

Scaling of morphology and ultrastructure of hearts among wild African antelope

Edward P. Snelling[1,*], Shane K. Maloney[1,2], Anthony P. Farrell[3,4], Leith C. R. Meyer[1,5], Adian Izwan[2], Andrea Fuller[1,5], Duncan Mitchell[1,2], Anna Haw[1], Mary-Ann Costello[6] and Roger S. Seymour[7]

ABSTRACT

The hearts of smaller mammals tend to operate at higher mass-specific mechanical work rates than those of larger mammals. The ultrastructural characteristics of the heart that allow for such variation in work rate are still largely unknown. We have used perfusion-fixation, transmission electron microscopy and stereology to assess the morphology and anatomical aerobic power density of the heart as a function of body mass across six species of wild African antelope differing by approximately 20-fold in body mass. The survival of wild antelope, as prey animals, depends on competent cardiovascular performance. We found that relative heart mass (g kg^{-1} body mass) decreases with body mass according to a power equation with an exponent of −0.12±0.07 (±95% confidence interval). Likewise, capillary length density (km cm^{-3} of cardiomyocyte), mitochondrial volume density (fraction of cardiomyocyte) and mitochondrial inner membrane surface density (m^2 cm^{-3} of mitochondria) also decrease with body mass with exponents of −0.17±0.16, −0.06±0.05 and −0.07±0.05, respectively, trends likely to be associated with the greater mass-specific mechanical work rate of the heart in smaller antelope. Finally, we found proportionality between quantitative characteristics of a structure responsible for the delivery of oxygen (total capillary length) and those of a structure that ultimately uses that oxygen (total mitochondrial inner membrane surface area), which provides support for the economic principle of symmorphosis at the cellular level of the oxygen cascade in an aerobic organ.

KEY WORDS: Capillarity, Cardiac, Mammal, Mitochondria, Myofibrils, Predation

INTRODUCTION

The size of the heart is determined by the magnitude of the volume loads and the pressure loads that act on the walls of the ventricles (Grande and Taylor, 1965; Seymour and Blaylock, 2000; White and Seymour, 2014). Heart mass increases with body mass principally because larger mammals have hearts that support a greater cardiac output and blood volume load compared with those of smaller mammals. This greater luminal capacity of the heart of larger mammals decreases the curvature of the ventricular walls, rendering larger hearts at a mechanical disadvantage that generally is compensated by a proportionate increase in ventricular wall thickness. Pressure loading is related to the prevailing arterial blood pressure, which increases slightly in larger mammals as a result of higher blood columns above the heart and is compensated by a proportionate increase in left ventricular wall thickness. According to the principle of Laplace, an increase in wall thickness ensures that overall average wall stress remains constant despite the increase in volume loading and pressure loading associated with increasing body mass.

The functional relationship between the heart and body size has lent itself to numerous scaling analyses, which generally have shown that heart mass increases in direct proportion to body mass (isometry) across diverse assemblages of mammalian species, with exponents of power equations relating heart mass to body mass in the range of 0.96 to 1.06 for eutherian mammals (Bishop, 1997; Brody, 1945; Holt et al., 1968; Hoppeler et al., 1984; Lindstedt and Schaeffer, 2002; Prothero, 1979; Seymour and Blaylock, 2000; Stahl, 1965) and 0.94 to 1.05 for marsupial mammals (Dawson and Needham, 1981; Dawson et al., 2003). Analyses within specific phylogenetic groups reinforce the isometric scaling of heart mass on body mass, with exponents of 0.95 in cetaceans (Prothero, 1979), 0.97 in primates (Stahl, 1965) and 1.03 in felids (Davis, 1962). However, an analysis of 13 species of antelope showed that heart mass increases with body mass with an exponent of only 0.88±0.10 (±95% confidence interval, CI), a value significantly less than isometry (Woodall, 1992). Thus, there exists the possibility that antelope, at least, deviate from the typical isometric scaling of heart mass on body mass. Analyses of heart mass within phylogenetic groups can reveal scaling patterns that are otherwise lost in larger interspecific examinations.

While some uncertainty remains regarding a universal scaling law for heart size in mammals, there is greater uncertainty about the scaling of the ultrastructural components of the heart that relate to myocardial oxygen supply and oxygen consumption. In particular, analysis of the scaling of the heart's capillary and mitochondrial components would be valuable because these structures are responsible for the delivery and consumption of oxygen in an organ that remains predominantly aerobic even during periods of maximum mechanical work (Snelling et al., 2016; Stanley et al., 2005). The only ultrastructure scaling analysis carried out to date showed that across 11 species of mammal, the heart's mitochondrial volume density scales with body mass according to a power equation with an exponent of −0.04±0.02, a value significantly less than zero (independent of body mass), and representing an appreciable decrease in mitochondrial volume density from 36.1% in a 2.4 g shrew to 21.1% in a 920 kg cow (Hoppeler et al., 1984).

[1]Brain Function Research Group, School of Physiology, University of the Witwatersrand, Johannesburg, Gauteng 2193, South Africa. [2]School of Human Sciences, University of Western Australia, Crawley, WA 6009, Australia. [3]Department of Zoology, University of British Columbia, Vancouver, BC, Canada V6T 1Z4. [4]Faculty of Land and Food Systems, University of British Columbia, Vancouver, BC, Canada V6T 1Z4. [5]Department of Paraclinical Sciences, University of Pretoria, Pretoria, Gauteng 0110, South Africa. [6]Central Animal Service, University of the Witwatersrand, Johannesburg, Gauteng 2193, South Africa. [7]School of Biological Sciences, University of Adelaide, Adelaide, SA 5005, Australia.

*Author for correspondence (edward.snelling@wits.ac.za)

E.P.S., 0000-0002-8985-8737; S.K.M., 0000-0002-5878-2266; L.C.R.M., 0000-0002-5122-2469; A.F., 0000-0001-6370-8151; D.M., 0000-0001-8989-4773; R.S.S., 0000-0002-3395-0059

Received 14 May 2018; Accepted 29 June 2018

Journal of Experimental Biology (2018) 221, jeb184713. doi:10.1242/jeb.184713

That same study found no systematic change with body mass in the mitochondrial inner membrane packing density, although it was based on a subset of only three species (the wood mouse, cat and cow). To our knowledge, there has been no analysis presented for the scaling of capillary density of the heart with body mass across different species of mammal. However, we do know that capillary density correlates linearly with mitochondrial volume density in hearts of 13 species of mammal (Hoppeler and Kayar, 1988). Indeed, this linear correlation between capillary density and mitochondrial volume density is evident in broader analyses incorporating the heart, diaphragm and several locomotor muscles of mammals (Conley et al., 1987; Hoppeler and Kayar, 1988; Hoppeler et al., 1981b; Hudlicka et al., 1992). The proportional relationship between an oxygen-delivery structure (capillaries) and an oxygen-consumption structure (mitochondria) lends support to the economic principle of symmorphosis, that structural design at each step of the oxygen cascade is commensurate with the functional capacity of the entire system (Weibel et al., 1998, 1991, 1992).

Despite the close functional association between capillaries and mitochondria, the apparent quantitative matching between these two structures does require further consideration (Bosutti et al., 2015; Egginton and Gaffney, 2010). For instance, the linear covariance between capillary density and mitochondrial volume density may be influenced by capillary measurements that are sensitive to scaling effects of fibre cross-sectional area (Egginton and Gaffney, 2010). Also, whereas mitochondrial volume density is probably associated directly with just the volume-specific aerobic capacity of the muscle, capillary density is probably associated with aerobic capacity, substrate delivery rate and metabolite removal rate, and the degree to which each function governs capillary density and distribution will probably vary depending on the situation. Thus, while it is true that capillary density generally covaries in a linear manner with mitochondrial volume density (Hoppeler and Kayar, 1988), it is also true that some glycolytic fibres have capillary densities that appear to be in excess of the fibre's maximum oxygen requirements (Gray and Renkin, 1978; Schmidt-Nielsen and Pennycuik, 1961), with the apparent excess capillary supply thought to be necessary to remove lactate (Hudlicka et al., 1987). Finally, capillary density alone may not accurately reflect oxygen supply to the mitochondria in instances where there is variation in the oxygen carrying capacity of the blood or myoglobin concentration of the surrounding fibres (Hoppeler and Kayar, 1988). For example, athletic mammals tend to have higher haematocrit during exercise than do non-athletic mammals, allowing them to achieve higher oxygen supply rates to the mitochondria with relatively fewer capillaries (Conley et al., 1987). Importantly, many of these caveats can be controlled through careful experimental design.

We set out to assess the morphology and anatomical aerobic power density of the heart as a function of body mass in six species of wild African antelope, prey animals that depend on competent cardiovascular performance for survival. Because the heart is an aerobic organ, we expected the role of the capillaries in the delivery of oxygen to be the driving design feature. By investigating wild antelope, we aimed to reduce some of the confounding effects caused by mixing athletic with non-athletic mammals. We combined gross ventricular dissection, perfusion-fixation, transmission electron microscopy and stereological analysis to derive scaling relationships for relative heart mass, capillary length density, mitochondrial volume density, mitochondrial inner membrane surface area relative to mitochondrial volume, and mitochondrial inner membrane surface area relative to cardiomyocyte volume. Because the capillaries serve oxygen delivery and the mitochondria serve oxygen consumption of the heart, we also test the relationship between total capillary length and total mitochondrial inner membrane surface area, seeking evidence for or against the principle of symmorphosis.

MATERIALS AND METHODS

Animals

All procedures were approved by the animal ethics committees of the University of the Witwatersrand (2015/04/11/A), University of Pretoria (V051/15) and University of Western Australia (RA/3/100/1340). The morphology and ultrastructure of the left and right ventricles of the heart were investigated in six species of wild African antelope, encompassing a ∼20-fold body mass range, and comprising the following in order of body mass: common duiker *Sylvicapra grimmia* (Linnaeus 1758) (*N*=3, 12–15 kg), springbok *Antidorcas marsupialis* (Zimmermann 1780) (*N*=3, 23–25 kg), blesbok *Damaliscus pygargus* (Pallas 1767) (*N*=3, 49–60 kg), gemsbok *Oryx gazella* (Linnaeus 1758) (*N*=3, 107–121 kg), blue wildebeest *Connochaetes taurinus* (Burchell 1823) (*N*=3, 131–177 kg) and common eland *Taurotragus oryx* (Pallas 1766) (*N*=3, 172–232 kg). All antelope were non-breeding adult females (*N*=18 individuals in total). The antelope were acquired from wild stock in their natural habitats in South Africa by darting with the immobilizing agent etorphine hydrochloride (M99, 0.05 mg kg^{-1} i.m.; Roche Products, Johannesburg, South Africa) and the tranquilizer azaperone (0.5 mg kg^{-1} i.m.; Roche Products). Once immobilized, the antelope were transported by utility vehicle to large outdoor enclosures (bomas), where they were housed for 3–6 weeks, and supplied with lucerne hay (alfalfa, *Medicago sativa*) and water *ad libitum*. Each antelope was inspected daily by a veterinarian. Each antelope was fasted 12–24 h before euthanasia (see below) and its body mass at euthanasia was recorded to the nearest 1 kg on a calibrated digital strain gauge scale (PCE-CS 5000N; PCE Instruments, Southampton, UK).

Chemical fixation of the heart

On the day of euthanasia, the antelope were darted with etorphine and azaperone at the same dosages used for initial capture, transported to a nearby operating theatre and given a lethal dose of pentobarbital (200 mg kg^{-1} i.v.; Kyron Laboratories, Johannesburg, South Africa). We then fixed their hearts chemically using solutions that we had established for sheep and goat hearts (Snelling et al., 2016). We made no attempt to fix the heart in a particular state of contraction. The thoracic cavity was opened and the ascending aorta cannulated retrogradely so that the cannula tip lay immediately above the entrance to the coronary arteries. A ligature around the aorta sealed the cannula in place. The coronary vascular system was perfused by gravity from a container 1.5 m above the level of the heart. Perfusate drained through an incision in the right atrial wall. Ringer's solution containing lidocaine (0.5 mg ml^{-1}) and heparin (20 IU ml^{-1}) was perfused until blood was cleared. This was followed by a fixative solution of 2.5% glutaraldehyde and 1.5% paraformaldehyde in 0.13 mol l^{-1} phosphate+0.02 mol l^{-1} sucrose buffer (320 mOsmol, pH 7.4; ADI Scientific, Johannesburg, South Africa) until the entire myocardium was firm. A ∼1 mm thick transmural strip of cardiac tissue was excised from two random locations within the left ventricular wall, and from one random location within the right ventricular wall. Each strip was immersed under a shallow layer of the same fixative solution and cut into at least 10 ∼1 mm^3 tissue blocks. One of those tissue blocks was selected randomly from each of the three strips for further processing. The block was immersed in the same fixative solution

Journal of Experimental Biology (2018) 221, jeb184713. doi:10.1242/jeb.184713

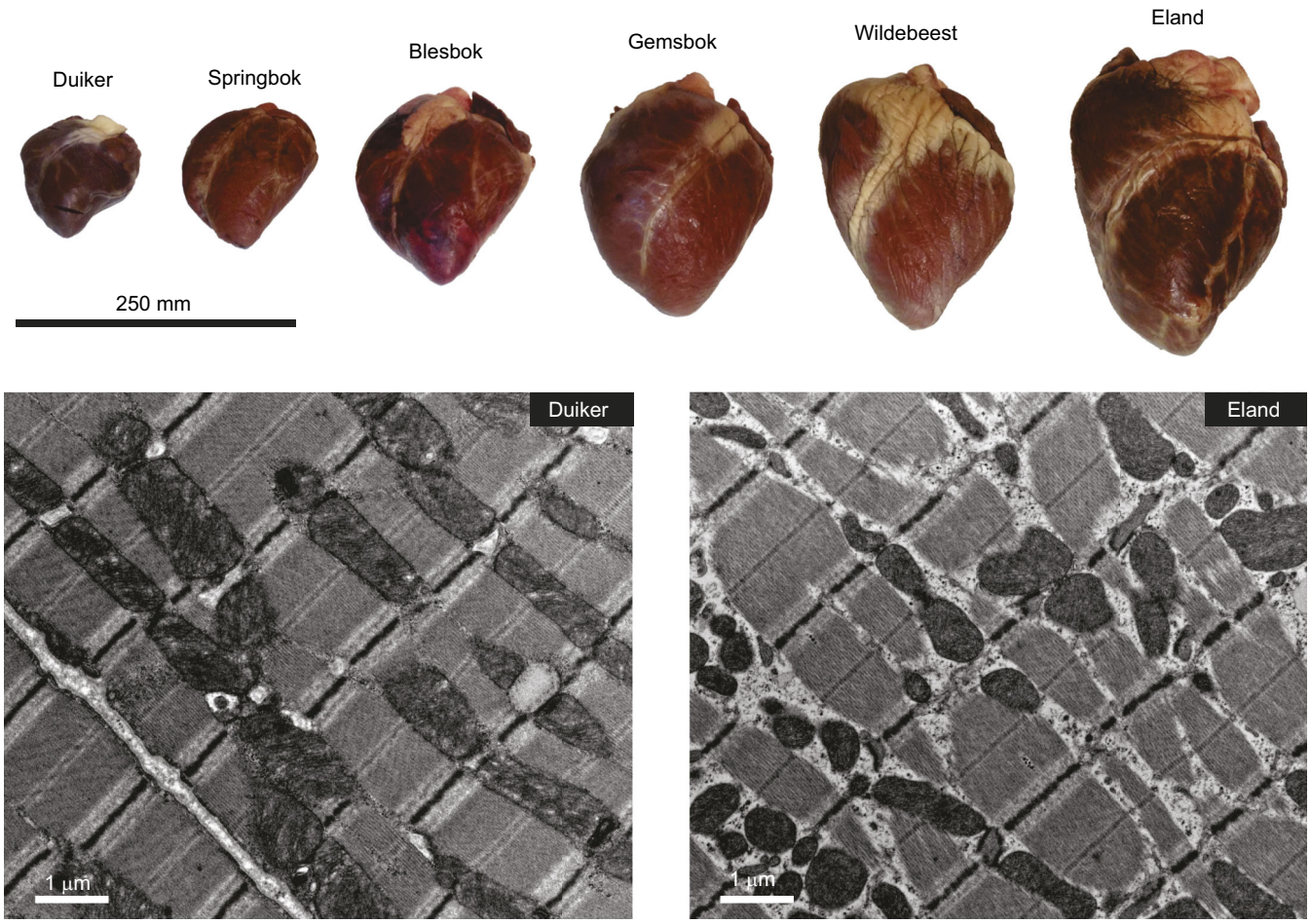

Fig. 1. Variation in the size and ultrastructure of the hearts of antelope. Whole hearts of the six species of wild African antelope, with transmission electron micrographs of the cardiomyocytes of the smallest (duiker) and largest species (eland).

for 3 days and then transferred to a solution of the same 0.15 mol l^{-1} phosphate–sucrose buffer for 3–6 days. Each block was then rinsed with the buffer (6×10 min) before secondary fixation in a 2% solution of osmium tetroxide (3 h). The block then was rinsed with distilled water (3×10 min) and dehydrated progressively by immersion in an ethanol series (50%, 60%, 70% and 80% for 10 min each), followed by immersion in 90% ethanol, 100% ethanol and propylene oxide (2×10 min each). The blocks then were gradually infiltrated with an embedding resin (Araldite-Embed kit; Electron Microscopy Sciences, Hatfield, PA, USA) at ratios of 3:1, 2:2 and 1:3 (propylene oxide:resin) and left overnight in pure resin. The following day, each block was submerged with random orientation into an individual embedding mould pre-filled with pure resin, and left to polymerize for 48 h in a 70°C oven.

Morphology and ultrastructure of the heart

After tissue sampling, the hearts were trimmed of visible fat, rinsed with an isotonic saline solution (0.90% w/v NaCl), and the chambers dissected and weighed to 0.1 g on an analytical balance (RP-300; Sauter, Balingen, Germany). We excised the left ventricular free wall plus septum ('left ventricle'), and the right ventricular free wall ('right ventricle'), consistent with our previous studies (Snelling et al., 2015a,b, 2016). The left and right ventricular tissue volumes (V_t; cm^3) were calculated as $V_t=M_t\rho_t^{-1}$, where M_t is the ventricular tissue mass (g) and ρ_t is the cardiac tissue mass density (~1.06 g cm^{-3}; Vinnakota and Bassingthwaighte, 2004). Unbiased estimates of the left and right ventricular ultrastructure were obtained from the fixed samples of cardiac tissue by generating isotropic uniform random (IUR) images for stereological analysis (Howard and Reed, 1998; Mühlfeld et al., 2010). An IUR image has a plane that is of uniform random position within the object from which it has been sampled (chapters 1 and 2 of Howard and Reed, 1998), and is perpendicular to an isotropic orientation within that object (chapters 6 and 7 of Howard and Reed, 1998). In practice, an IUR image is achieved by uniform random sampling at each level of the sampling hierarchy, and by randomizing section position and angle in 3D space. To this end, a 70 nm ultrathin section was cut at a random depth and orientation from each sample using an 8 mm glass knife, a 2.4 mm diamond knife (Ultra 45°; Diatome, Nidau, Switzerland) and an ultramicrotome (EM UC6; Leica Microsystems, Wetzlar, Germany). Ultrathin sections were placed onto 3 mm copper mesh grids, stained with uranyl acetate (15 min) and lead citrate (10 min), and viewed with a 100 kV transmission electron microscope (Tecnai G2; FEI, Hillsboro, OR, USA) coupled to an in-column charged-couple device digital camera (Veleta; Olympus, Tokyo, Japan). We moved systematically along the length and breadth of each section, capturing 10 random images of ventricular tissue (×1700), cardiomyocyte ultrastructure (×11,500), capillaries (×6000) and mitochondria (×60,000).

The images were imported into a computer graphics program (CorelDraw 15; Corel Corporation, Ottawa, ON, Canada), where the images of the ventricular tissue were analysed with a lattice

Table 1. Scaling of heart mass and of heart cardiomyocyte volume density and cardiomyocyte volume across six species of wild African antelope (~20-fold body mass range; *N*=18 individuals)

	Heart*	LV	RV	LV versus RV ANCOVA slope (elevation)
Relative mass (g kg^{-1} M_b)	$8.21M_b^{-0.12\pm0.07}$ r^2=0.44, P=0.0027	$5.77M_b^{-0.11\pm0.06}$ r^2=0.44, P=0.0027	$2.47M_b^{-0.16\pm0.11}$ r^2=0.37, P=0.0076	$F_{1,32}$=0.74, P=0.40 ($F_{1,33}$=323, P<0.0001)
Absolute mass (g)	$8.21M_b^{0.88\pm0.07}$ r^2=0.98, P<0.0001	$5.77M_b^{0.89\pm0.06}$ r^2=0.98, P<0.0001	$2.47M_b^{0.84\pm0.11}$ r^2=0.94, P<0.0001	$F_{1,32}$=0.74, P=0.40 ($F_{1,33}$=323, P<0.0001)
Cardiomyocyte volume density (fraction of cardiac tissue)	$0.769M_b^{0.03\pm0.03}$ r^2=0.26, P=0.030	$0.785M_b^{0.03\pm0.04}$ r^2=0.13, P=0.14	$0.739M_b^{0.04\pm0.03}$ r^2=0.35, P=0.0098	$F_{1,32}$=0.34, P=0.57 ($F_{1,33}$=0.19, P=0.67)
Cardiomyocyte volume (cm^3)	$5.99M_b^{0.91\pm0.09}$ r^2=0.97, P<0.0001	$4.27M_b^{0.92\pm0.09}$ r^2=0.97, P<0.0001	$1.72M_b^{0.88\pm0.13}$ r^2=0.93, P<0.0001	$F_{1,32}$=0.29, P=0.59 ($F_{1,33}$=224, P<0.0001)

Scaling of the left ventricular (LV) and right ventricular (RV) chambers is also shown with ANCOVA comparisons of slope and elevation (in parentheses) for each variable.

Scaling equations are in the form $y=aM_b^{b\pm95\%CI}$ where y is the variable of interest, a is the scaling coefficient (elevation), b is the scaling exponent (slope of the log-transformed relationship), M_b is body mass in kg, and CI stands for confidence interval.

*Heart represents the ventricular chambers only. Including the ventricular and atrial chambers, relative heart mass follows the equation $y=9.35M_b^{-0.13\pm0.07}$, r^2=0.46, P=0.0019, and absolute heart mass follows the equation $y=9.35M_b^{0.87\pm0.07}$, r^2=0.98, P<0.0001.

of grid points superimposed randomly, with the relative number of points falling on cardiomyocyte fibres and capillaries (lumen+endothelium) counted. The total volumes of the cardiomyocyte fibre and capillary structures (V_s; cm^3) were calculated as $V_s=V_{V(s,t)}V_t$, where $V_{V(s,t)}$ is the fraction of ventricular tissue occupied by the structure determined from the grid point counts (Cruz-Orive and Weibel, 1990; Mayhew, 1991). Images of cardiomyocyte ultrastructure were also analysed with a lattice of grid points superimposed randomly, and the relative number of points hitting myofibril and mitochondrion organelles counted. Total myofibril and mitochondrial organelle volumes (V_o; cm^3) were calculated as $V_o=V_{V(o,f)}V_f$, where $V_{V(o,f)}$ is the fraction of cardiomyocyte fibre occupied by the organelle determined from the grid point counts, and V_f is the total cardiomyocyte fibre volume (cm^3). Images of mitochondria were analysed with an isotropic Merz grid superimposed randomly, with the ratio of mitochondrial inner membrane surface area to mitochondrial volume ($S_{V(im,mt)}$; m^2 cm^{-3} of mitochondria) calculated as $S_{V(im,mt)}=2I/l^{-1}\times10^{-4}$, where I is the number of intersections of the test lines with the inner membrane surface, l is the total length (cm) of test lines falling over the mitochondrion, and $\times10^{-4}$ converts to the conventional units of m^2 cm^{-3} (Cruz-Orive and Weibel, 1990; Mayhew, 1991). The total mitochondrial inner membrane surface area (S_{im}; m^2) was calculated as $S_{im}=S_{V(im,mt)}V_{mt}$, where V_{mt} is the total mitochondrial volume (cm^3). The ratio of mitochondrial inner membrane surface area to cardiomyocyte fibre volume ($S_{V(im,f)}$; m^2 cm^{-3} of cardiomyocyte) could then be calculated as $S_{V(im,f)}=S_{im}/V_f$. Lastly, we analysed aspects of the capillary–cardiomyocyte geometry (Egginton, 1990; Hudlicka et al., 1992; Mathieu-Costello, 1993; Olfert et al., 2016). We directly measured the cross-sectional radius of capillaries (R_c; μm) from the images. The mean number of capillary profiles per unit cross-sectional area of fibre ($N_{A(c,f)}$; mm^{-2} of cardiomyocyte) was then calculated as $N_{A(c,f)}=\pi^{-1}R_c^{-2}(V_f/V_c)^{-1}\times10^6$, where V_c is the total capillary volume (cm^3) and $\times10^6$ converts to the conventional units of mm^{-2}. This assumes that capillaries are a perfect cylinder. Finally, total capillary length (J_c; km) was calculated as $J_c=V_c(\pi R_c^2)^{-1}\times10^3$, where $\times10^3$ converts length to units of km, and the ratio of capillary length to cardiomyocyte fibre volume ($J_{V(c,f)}$; km cm^{-3} of cardiomyocyte) was calculated as $J_{V(c,f)}=J_c/V_f$.

Statistical analyses

Scaling relationships were obtained by calculating ordinary least-squares linear regressions of $\log_{10}$-transformed data with body mass as the independent variable (Kilmer and Rodríguez, 2017; Smith, 2009). An F-test assessed the statistical significance of the correlation, and the coefficient of determination (r^2) evaluated its strength. An ANCOVA tested for significant differences in slope (scaling exponent) and in elevation (scaling coefficient) between regressions (Zar, 1998). Although statistical analyses were performed on $\log_{10}$-transformed data, we report the scaling relationships in the form of a power equation, $y=aM_b^{b\pm95\%CI}$, where y is the variable of interest, a is the scaling coefficient, b is the scaling exponent, M_b is body mass in kg and CI stands for confidence interval. Statistical significance was set at 0.05 *a priori*

Table 2. Scaling of heart capillary network across six species of wild antelope (*N*=18)

	Heart*	LV	RV	LV versus RV ANCOVA slope (elevation)
Capillary volume density (fraction of cardiac tissue)	$0.200M_b^{0.25\pm0.17}$ r^2=0.40, P=0.0051	$0.208M_b^{0.26\pm0.21}$ r^2=0.31, P=0.016	$0.173M_b^{0.24\pm0.22}$ r^2=0.25, P=0.033	$F_{1,32}$=0.030, P=0.86 ($F_{1,33}$=0.38, P=0.54)
Capillary volume (cm^3)	$1.56M_b^{0.62\pm0.14}$ r^2=0.85, P<0.0001	$1.13M_b^{0.63\pm0.17}$ r^2=0.79, P<0.0001	$0.40M_b^{0.60\pm0.20}$ r^2=0.73, P<0.0001	$F_{1,32}$=0.048, P=0.83 ($F_{1,33}$=92, P<0.0001)
Capillary numerical density (mm^{-2} of cardiomyocyte)	$7631M_b^{-0.17\pm0.16}$ r^2=0.24, P=0.039	$7945M_b^{-0.18\pm0.15}$ r^2=0.27, P=0.028	$5938M_b^{-0.14\pm0.31}$ r^2=0.06, P=0.34	$F_{1,32}$=0.038, P=0.85 ($F_{1,33}$=1.00, P=0.33)
Capillary length density (km cm^{-3} of cardiomyocyte)	$7.63M_b^{0.17\pm0.16}$ r^2=0.24, P=0.039	$7.94M_b^{0.18\pm0.15}$ r^2=0.27, P=0.028	$5.94M_b^{0.14\pm0.31}$ r^2=0.06, P=0.34	$F_{1,32}$=0.038, P=0.85 ($F_{1,33}$=1.00, P=0.33)
Total capillary length (km)	$45.45M_b^{0.74\pm0.16}$ r^2=0.85, P<0.0001	$33.96M_b^{0.74\pm0.18}$ r^2=0.82, P<0.0001	$10.22M_b^{0.74\pm0.24}$ r^2=0.72, P<0.0001	$F_{1,32}$=0.0029, P=0.96 ($F_{1,33}$=78, P<0.0001)

Estimates for the capillary network are associated with broad exponent confidence intervals in part because we did not fix the heart in a particular state of contraction and, as such, encountered varying states of vessel compression, as would be experienced across the cardiac cycle. Reaction to aldehyde perfusion may have contributed to this variation. See Table 1 for abbreviations, and regression and statistical details.

*Heart represents the ventricular chambers only.

Table 3. Scaling of heart myofibril and mitochondrial complement across six species of wild antelope (*N*=18)

	Heart*	LV	RV	LV versus RV ANCOVA slope (elevation)
Myofibril volume density (fraction of cardiomyocyte)	$0.645M_b^{0.00\pm0.03}$ r^2=0.00, P=0.83	$0.644M_b^{0.00\pm0.03}$ r^2=0.00, P=0.94	$0.646M_b^{0.01\pm0.04}$ r^2=0.01, P=0.70	$F_{1,32}$=0.064, P=0.80 ($F_{1,33}$=0.89, P=0.35)
Myofibril volume (cm^3)	$3.87M_b^{0.91\pm0.08}$ r^2=0.98, P<0.0001	$2.75M_b^{0.92\pm0.08}$ r^2=0.98, P<0.0001	$1.11M_b^{0.87\pm0.11}$ r^2=0.94, P<0.0001	$F_{1,32}$=0.49, P=0.49 ($F_{1,33}$=298, P<0.0001)
Mitochondrial volume density (fraction of cardiomyocyte)	$0.266M_b^{-0.06\pm0.05}$ r^2=0.30, P=0.018	$0.251M_b^{-0.05\pm0.05}$ r^2=0.20, P=0.064	$0.299M_b^{-0.08\pm0.07}$ r^2=0.30, P=0.018	$F_{1,32}$=0.63, P=0.43 ($F_{1,33}$=1.30, P=0.26)
Mitochondrial volume (cm^3)	$1.57M_b^{0.85\pm0.11}$ r^2=0.94, P<0.0001	$1.07M_b^{0.87\pm0.11}$ r^2=0.94, P<0.0001	$0.51M_b^{0.80\pm0.15}$ r^2=0.89, P<0.0001	$F_{1,32}$=0.65, P=0.43 ($F_{1,33}$=140, P<0.0001)

See Table 1 for abbreviations, and regression and statistical details.
*Heart represents the ventricular chambers only.

and all analyses were performed using statistical software (Prism 6; GraphPad Software, La Jolla, CA, USA).

RESULTS

The size and ultrastructure of the heart differed significantly between the species of antelope examined in this study (Fig. 1). Full scaling equations and their statistics are presented in Tables 1–4. Overall, the smaller species had relatively larger hearts, with anatomical structures potentially delivering greater aerobic power densities, than those of the larger species. These trends were evident in the negative scaling exponents for relative heart mass (−0.12±0.07, P=0.0027) (Fig. 2A), capillary length density (−0.17±0.16, P=0.039) (Fig. 2B), mitochondrial volume density (−0.06±0.05, P=0.018) (Fig. 2C), surface density of mitochondrial inner membrane per unit volume of mitochondria (−0.07±0.05, P=0.015) (Fig. 2D) and surface density of mitochondrial inner membrane per unit volume of cardiomyocyte (−0.13±0.07, P=0.0013) (Fig. 2E). In each case, the exponent was significantly less than zero. We also found parallel scaling between an oxygen-delivery structure and an oxygen-consumption structure of the heart, with total capillary length scaling with an exponent of 0.74±0.16 (P<0.0001) (Fig. 3A), and total mitochondrial inner membrane surface area scaling with a statistically indistinguishable exponent of 0.78±0.10 (P<0.0001) (Fig. 3B) (ANCOVA; $F_{1,32}$=0.23, P=0.63), leading to linear covariance (proportionality) between total capillary length and total mitochondrial inner membrane surface area (Fig. 4).

When we examined the left and right ventricles of the heart separately, we saw similar scaling patterns for the various morphological and ultrastructural variables between the two chambers (Tables 1–4). Variables expressed in absolute terms, including ventricular mass, cardiomyocyte volume, capillary volume, total capillary length, myofibril volume, mitochondrial volume and mitochondrial inner membrane surface area, all scaled against body mass with exponents statistically indistinguishable between the left and right ventricles (ANCOVA; P>0.05), but all had significantly different elevations (P<0.05), driven by the larger size of the left ventricle compared with the right ventricle. Variables expressed in relative terms, including cardiomyocyte volume density, capillary density, myofibril and mitochondrial volume densities, and mitochondrial inner membrane surface density, all scaled against body mass with exponents and elevations statistically indistinguishable between the left and right ventricles (P>0.05).

DISCUSSION

Scaling is a powerful tool to assess variation in morphological and physiological traits as a function of body mass, especially when the derived relationships are compared among multiple traits that are related to one another. Our study on the scaling of the morphology and ultrastructure of the heart across six species of wild African antelope revealed three notable findings. First, the relative size of the heart of antelope decreases with increasing body mass. Second, the capillary length density, mitochondrial volume density and mitochondrial inner membrane packing density all decrease as body mass increases. Third, the total capillary length and total mitochondrial inner membrane surface area increase in parallel as body mass increases, meaning that there is linear covariance (proportionality) between a structure involved in the delivery of oxygen and a structure involved in oxygen consumption. We conclude that smaller antelope have a greater relative heart size and a higher density of aerobic power-generating structures than do larger antelope, and that there is economy in cardiac design in the matching of oxygen-delivery and oxygen-consumption structures.

Across the body size range of our antelope, heart mass increases with body mass with an exponent of 0.88±0.07, and thus relative heart mass decreases with body mass with an exponent of −0.12±0.07 (Fig. 2A). This finding is at odds with the isometric scaling of heart mass on body mass reported from broad interspecific analyses of mammals (Bishop, 1997; Brody, 1945; Prothero, 1979; Stahl, 1965), as well as narrower analyses of some phylogenetic groups (Davis, 1962; Prothero, 1979; Stahl, 1965). Nevertheless, our exponent of 0.88 is identical to that derived in an earlier study on 13 species of antelope (Woodall, 1992). Thus, we speculate that particular natural selective forces might be contributing to the pattern of decreasing relative heart size with increasing body mass in

Table 4. Scaling of heart mitochondrial inner membrane surface dimensions across six species of wild antelope (*N*=18)

	Heart*	LV	RV	LV versus RV ANCOVA slope (elevation)
Mitochondrial inner membrane surface density (m^2 cm^{-3} of mitochondria)	$47.91M_b^{-0.07\pm0.05}$ r^2=0.32, P=0.015	$49.31M_b^{-0.07\pm0.06}$ r^2=0.31, P=0.017	$44.75M_b^{-0.06\pm0.08}$ r^2=0.15, P=0.11	$F_{1,32}$=0.042, P=0.84 ($F_{1,33}$=1.76, P=0.19)
Mitochondrial inner membrane surface density (m^2 cm^{-3} of cardiomyocyte)	$12.74M_b^{-0.13\pm0.07}$ r^2=0.49, P=0.0013	$12.36M_b^{-0.12\pm0.07}$ r^2=0.45, P=0.0023	$13.38M_b^{-0.14\pm0.12}$ r^2=0.29, P=0.021	$F_{1,32}$=0.12, P=0.73 ($F_{1,33}$=0.048, P=0.83)
Mitochondrial inner membrane surface area (m^2)	$75.88M_b^{0.78\pm0.10}$ r^2=0.95, P<0.0001	$52.81M_b^{0.80\pm0.10}$ r^2=0.95, P<0.0001	$23.03M_b^{0.74\pm0.14}$ r^2=0.88, P<0.0001	$F_{1,32}$=0.57, P=0.46 ($F_{1,33}$=179, P<0.0001)

See Table 1 for abbreviations, and regression and statistical details.
*Heart represents the ventricular chambers only.

Journal of Experimental Biology (2018) 221, jeb184713. doi:10.1242/jeb.184713

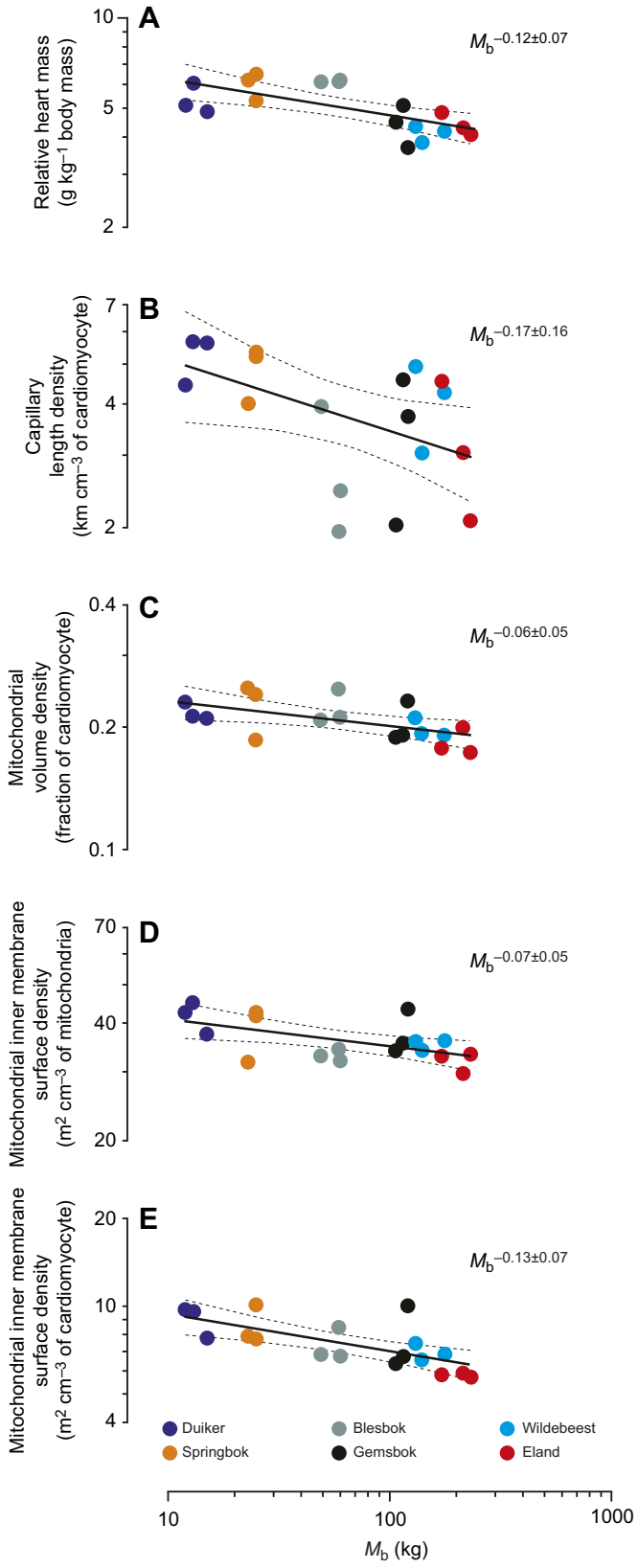

Fig. 2. Scaling of the anatomical aerobic power density of the hearts of antelope. Decreasing scaling relationships with increasing body mass are evident for (A) relative heart mass, (B) capillary length density, (C) mitochondrial volume density, (D) the surface density of mitochondrial inner membrane relative to mitochondrial volume and (E) the surface density of mitochondrial inner membrane relative to cardiomyocyte volume, across six species of wild African antelope (~20-fold body mass range; N=18 individuals). Scaling of these anatomical structures against heart mass (instead of body mass, M_b) produces very similar exponents. Solid line is the regression mean, dashed lines represent the 95% confidence band. See Tables 1–4 for complete scaling equations and their statistics.

African antelope. Because heart mass is related to volume loading, maximum cardiac output, pulmonary diffusing capacity and maximum sustainable aerobic exercise (Bishop, 1997), our results suggest that smaller antelope, including the blesbok, might have relatively higher sustainable aerobic capacities than do larger antelope. The relatively greater heart mass may arise partly as a consequence of predation pressure, as smaller antelope tend to be more vulnerable to a broader range of different-sized predators than larger antelope, which are normally vulnerable only to large predators and cooperative pack hunters (Hayward and Kerley, 2008; Jarman, 1974; Radloff and Du Toit, 2004).

In addition to confirming that smaller antelope have relatively larger hearts than do larger antelope, we also found that the smaller antelope have hearts that contain relatively greater capillary length densities and relatively greater mitochondrial volume densities, and that the mitochondria themselves have relatively greater inner membrane surface densities. These findings are manifest in the negative scaling exponents for capillary length density (−0.17±0.16; Fig. 2B), mitochondrial volume density (−0.06±0.05; Fig. 2C) and mitochondria inner membrane surface density (−0.07±0.05; Fig. 2D). Overall, these scaling relationships imply that the hearts of smaller antelope also have the anatomical potential for a greater aerobic power density. Our value for the exponent of the power equation relating mitochondrial volume density to body mass (−0.06) is similar to the value obtained from a broader interspecific assessment of the hearts of 11 species of mammal (−0.04±0.02) (Hoppeler et al., 1984). However, that same assessment analysed the inner membrane packing density of the mitochondria in a subset of three species (the wood mouse, cat and cow) and found no systematic change with body mass, while we found a negative power relationship with body mass, with an exponent of −0.07. More species and more randomly sectioned mitochondria would need to be analysed to determine whether the inner membrane surface density varies with body mass generally in mammals. Nonetheless, the need to accommodate matrix enzymes between the cristae probably imposes an upper limit on mitochondrial inner membrane surface density (Suarez, 1996). As far as we know, locomotor skeletal muscle is the only other tissue upon which similar scaling analyses have been performed, and in those studies capillary numerical density scaled with body mass with an exponent of −0.11 (Hoppeler et al., 1981b) while mitochondrial volume density scaled with an exponent of −0.18 (Mathieu et al., 1981). Thus, there seems to be a general trend for greater mitochondrial and capillary investment in tissues of smaller mammals. There is no consensus on an underlying explanation for this trend. Nonetheless, we note the inherently higher mass-specific metabolic rates of smaller mammals compared with those of larger ones.

Another important finding from our study relates to the apparent proportional investment between the capillaries and the mitochondria of the heart. By focusing our analysis on the aerobic tissue of the heart, we assume the primary role of the capillaries is that of oxygen delivery, and by restricting our analysis to wild prey animals, we attempted to limit some of the confounding effects caused by mixing athletic with non-athletic mammals. Total capillary length is a morphometric descriptor of global

Journal of Experimental Biology (2018) 221, jeb184713. doi:10.1242/jeb.184713

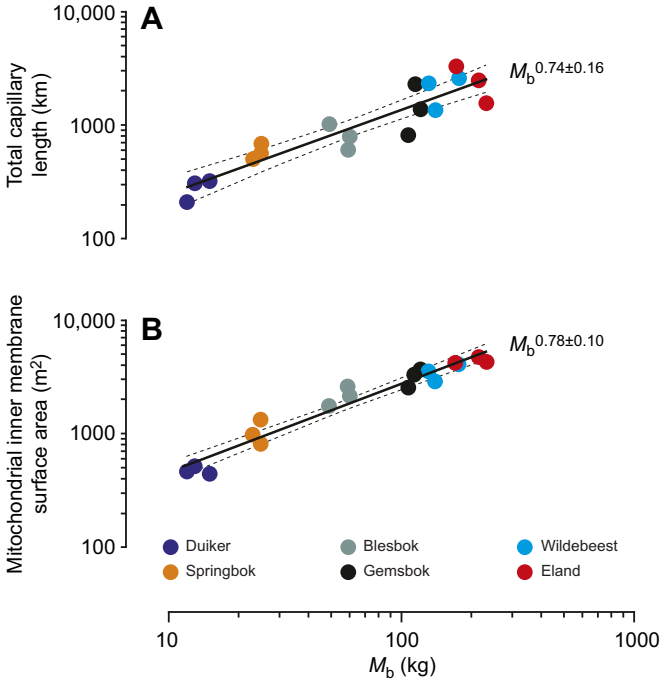

Fig. 3. Parallel scaling of the oxygen-delivery and oxygen-consumption apparatus of the hearts of antelope. The statistically indistinguishable scaling exponents for (A) total capillary length and (B) total mitochondrial inner membrane surface area, in a power curve on body mass, is evidence of economy in cardiac design (symmorphosis) across six species of wild African antelope (N=18 individuals). Solid line is the regression mean, dashed lines represent the 95% confidence band. See Tables 2 and 4 for complete scaling equations and their statistics.

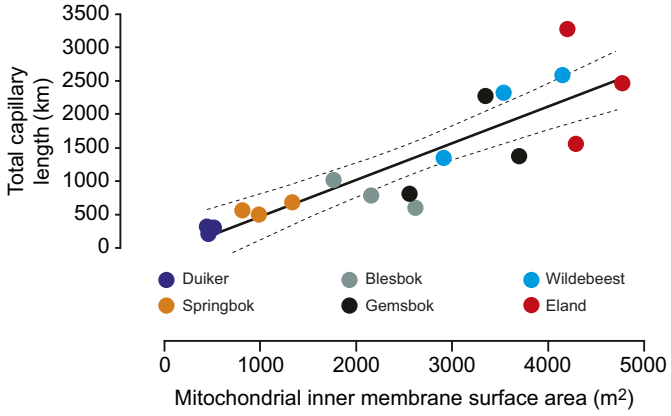

Fig. 4. Proportionality between the oxygen-delivery and oxygen-consumption apparatus of the hearts of antelope. The linear covariance between total capillary length (J_c; km) and total mitochondrial inner membrane surface area (S_{im}; m^2) is evidence of symmorphosis across six species of wild African antelope (N=18 individuals). Linear regression equation J_c=−79.7+0.55S_{im} (r^2=0.75, P<0.0001). Solid line is the regression mean, dashed lines represent the 95% confidence band.

oxygen-supply capacity because it is linked with total capillary blood volume, total capillary endothelial surface area and average oxygen diffusion distance to the mitochondria (Hoppeler and Kayar, 1988; Hoppeler et al., 1981b). Likewise, total mitochondrial inner membrane surface area is a morphometric descriptor of global oxygen-consumption capacity, because it is on the inner membrane that the enzymes of oxidative phosphorylation are embedded and where oxygen ultimately is consumed at the final step of the electron transport chain (Hoppeler and Kayar, 1988; Hoppeler et al., 1981a). It is significant, then, that we find proportionality between these two variables for the heart, implied by the parallel scaling of total capillary length (exponent 0.74±0.16; Fig. 3A) and total mitochondrial inner membrane surface area (exponent 0.78±0.10; Fig. 3B), and demonstrated by their linear covariance (Fig. 4). This proportionality conforms to the economic design principle of symmorphosis, which posits that no more structure should exist in a system, including the steps of the oxygen cascade, than is necessary to satisfy the functional capacity of the system, assuming the driving design feature is the transport of oxygen. The functional aerobic capacity of the heart, a state that is probably approached during heavy aerobic exercise, should be reflected in the global maximum oxygen-consumption rate of the cardiac tissue. Symmorphosis would also predict that the maximum oxygen-consumption rate of the antelope heart should scale in parallel with total capillary length and total mitochondrial inner membrane surface area – that is, with an exponent of ca. 0.74–0.78 in a power equation on body mass. We cannot yet test this hypothesis directly because data for the aerobic capacity of cardiac tissue in our antelope are unavailable. Nonetheless, if the scaling of heart mass is associated with stroke work (≈stroke volume×mean arterial blood pressure), then stroke work would be predicted to scale with an exponent of 0.88, and if maximum heart rate scales with an exponent of −0.16, as it does across broader interspecific analyses of mammals (Bishop, 1997), then assuming the heart's metabolic to mechanical energy conversion efficiency is independent of body mass, we would expect the antelope heart's maximum oxygen-consumption rate to scale with an exponent of 0.88–0.16=0.72, not far off the scaling of 0.74–0.78 obtained for the structures that support this cardiac work.

Further evidence for symmorphosis at the cellular level of cardiac design for the oxygen cascade is provided by mathematical modelling that shows perfusion and cardiac capillary investment are sufficient to satisfy approximately 90% of the heart's maximum oxygen requirements, and that cardiac mitochondria operate within 80% of their capacity when the heart is working near its functional limits during simulated heavy exercise (Snelling et al., 2016). Adequate perfusion and a proportionate investment of cardiac capillaries is further implied by evidence that shows lactate release from the myocardium is relatively modest during exercise (Gertz et al., 1981, 1988; van Hall, 2010). Indeed, the healthy non-ischaemic myocardium is a net consumer of circulating lactate even when the heart is operating close to its normal maximum power output (Kaijser and Berglund, 1992; Massie et al., 1994; Stanley et al., 2005). Also of relevance is the unique physiology and anatomy of birds that fly at high altitude, which have adapted multiple steps of the oxygen cascade, from the lungs to the working muscles, to enhance oxygen uptake, delivery and consumption, to sustain energy-intensive flight under low-oxygen partial pressure and reduced air density (Petschow et al., 1977; Scott, 2011; Scott et al., 2009, 2015; Scott and Milsom, 2007). However, there is evidence that the augmentation in oxygen supply is not necessarily in proportion to oxygen demand, particularly in reference to the heart, violating the principle of symmorphosis. The ventricular myocardium of high-altitude bar-headed geese has a higher capillary density, but not a higher citrate synthase activity (a marker of mitochondrial abundance), than that of low-altitude pink-footed geese and barnacle geese (Scott et al., 2011). One explanation for this apparent over-supply of capillaries is that it is an

adaptation contributing to the maintenance of oxygen partial pressure in the cardiomyocytes of bar-headed geese when flying at high altitude. Nonetheless, this example does serve to reinforce that we need circumspection in our interpretation of matching between capillary and mitochondrial investment (Egginton and Gaffney, 2010; Hoppeler and Kayar, 1988), even in aerobic organs like the heart.

In summary, we found that the relative size of the heart decreases with body mass across six species of wild African antelope. We also found that the heart's capillary length density, mitochondrial volume density and mitochondrial inner membrane packing density decrease with body mass, a trend which we think is related to the inherently higher mass-specific metabolic rates of tissue in smaller than in larger mammals. Lastly, we found proportionality between the capillary and mitochondrial inner membrane investments of the heart, which is evidence for quantitative matching between the oxygen-delivery structures and the oxygen-consumption structures, and is consistent with the principle of symmorphosis.

Acknowledgements
The authors gratefully acknowledge the expertise and contribution made by members of the School of Physiology, and the Central Animal Service, University of the Witwatersrand, especially David Gray, Gavin Norton, Tapiwa Chinaka, Zipho Zwane, Robyn Hetem and W. Maartin Strauss. We also acknowledge two anonymous reviewers for their valuable suggestions on an earlier draft.

Competing interests
The authors declare no competing or financial interests.

Author contributions
Conceptualization: R.S.S.; Methodology: E.P.S., S.K.M., A.P.F., L.C.M., A.F., D.M., A.H., M.C., R.S.S.; Software: E.P.S., S.K.M., L.C.M., A.F., D.M., R.S.S.; Validation: E.P.S., S.K.M., A.P.F., L.C.M., R.S.S.; Formal analysis: E.P.S.; Investigation: E.P.S., S.K.M., A.P.F., L.C.M., A.I., A.F., D.M., A.H., M.C., R.S.S.; Resources: E.P.S., S.K.M., A.P.F., L.C.M., A.F., D.M., A.H., M.C., R.S.S.; Data curation: E.P.S.; Writing - original draft: E.P.S.; Writing - review & editing: E.P.S., S.K.M., A.P.F., L.C.M., A.I., A.F., D.M., A.H., M.C., R.S.S.; Visualization: E.P.S., S.K.M., A.P.F., L.C.M., A.I., A.F., D.M., A.H., M.C., R.S.S.; Supervision: E.P.S., S.K.M., A.P.F., L.C.M., R.S.S.; Project administration: S.K.M., A.P.F., R.S.S.; Funding acquisition: E.P.S., S.K.M., A.P.F., R.S.S.

Funding
This research was supported by an Australian Research Council Discovery Project Award to R.S.S., S.K.M. and A.P.F. [DP-120102081], a South African Claude Leon Foundation Postdoctoral Fellowship to E.P.S., and a Natural Sciences and Engineering Research Council of Canada Discovery Grant to A.P.F.

Data availability
Raw data are available from ResearchGate: www.researchgate.net/profile/Edward_Snelling.

References
Bishop, C. M. (1997). Heart mass and the maximum cardiac output of birds and mammals: Implications for estimating the maximum aerobic power input of flying animals. *Philos. Trans. R. Soc. Lond. B. Biol. Sci.* **352**, 447-456.
Bosutti, A., Egginton, S., Barnouin, Y., Ganse, B., Rittweger, J. and Degens, H. (2015). Local capillary supply in muscle is not determined by local oxidative capacity. *J. Exp. Biol.* **218**, 3377-3380.
Brody, S. (1945). *Bioenergetics and Growth: With Special Reference to the Efficiency Complex in Domestic Animals*. New York: Reinhold Publishing Corporation.
Conley, K. E., Kayar, S. R., Rösler, K., Hoppeler, H., Weibel, E. R. and Taylor, C. R. (1987). Adaptive variation in the mammalian respiratory system in relation to energetic demand: IV. Capillaries and their relationship to oxidative capacity. *Respir. Physiol.* **69**, 47-64.
Cruz-Orive, L. M. and Weibel, E. R. (1990). Recent stereological methods for cell biology: a brief survey. *Am. J. Physiol. Lung Cell. Mol. Physiol.* **258**, L148-L156.
Davis, D. D. (1962). Allometric relationships in lions vs. domestic cats. *Evolution* **16**, 505-514.
Dawson, T. J. and Needham, A. D. (1981). Cardiovascular characteristics of two resting marsupials: An insight into the cardio-respiratory allometry of marsupials. *J. Comp. Physiol.* **145**, 95-100.
Dawson, T. J., Webster, K. N., Mifsud, B., Raad, E., Lee, E. and Needham, A. D. (2003). Functional capacities of marsupial hearts: size and mitochondrial parameters indicate higher aerobic capabilities than generally seen in placental mammals. *J. Comp. Physiol. B* **173**, 583-590.
Egginton, S. (1990). Morphometric analysis of tissue capillary supply. In *Advances in Comparative and Environmental Physiology*, Vol. 6 (ed. R. G. Boutilier), pp. 73-141. Berlin: Springer-Verlag.
Egginton, S. and Gaffney, E. (2010). Tissue capillary supply–it's quality not quantity that counts! *Exp. Physiol.* **95**, 971-979.
Gertz, E. W., Wisneski, J. A., Neese, R., Bristow, J. D., Searle, G. L. and Hanlon, J. T. (1981). Myocardial lactate metabolism: evidence of lactate release during net chemical extraction in man. *Circulation* **63**, 1273-1279.
Gertz, E. W., Wisneski, J. A., Stanley, W. C. and Neese, R. A. (1988). Myocardial substrate utilization during exercise in humans: dual carbon-labeled carbohydrate isotope experiments. *J. Clin. Invest.* **82**, 2017-2025.
Grande, F. and Taylor, H. L. (1965). Adaptive changes in the heart, vessels, and patterns of control under chronically high loads. In *Handbook of Physiology, Sec. 2: Circulation*, Vol. 3 (ed. W. F. Hamilton), pp. 2615-2677. Washington D.C: American Physiological Society.
Gray, S. D. and Renkin, E. M. (1978). Microvascular supply in relation to fiber metabolic type in mixed skeletal muscles of rabbits. *Microvasc. Res.* **16**, 406-425.
Hayward, M. W. and Kerley, G. I. H. (2008). Prey preferences and dietary overlap amongst Africa's large predators. *S. Afr. J. Wildl. Res.* **38**, 93-108.
Holt, J. P., Rhode, E. A. and Kines, H. (1968). Ventricular volumes and body weight in mammals. *Am. J. Physiol.* **215**, 704-715.
Hoppeler, H. and Kayar, S. R. (1988). Capillarity and oxidative capacity of muscles. *News Physiol. Sci.* **3**, 113-116.
Hoppeler, H., Mathieu, O., Krauer, R., Claassen, H., Armstrong, R. B. and Weibel, E. R. (1981a). Design of the mammalian respiratory system: VI. Distribution of mitochondria and capillaries in various muscles. *Respir. Physiol.* **44**, 87-111.
Hoppeler, H., Mathieu, O., Weibel, E. R., Krauer, R., Lindstedt, S. L. and Taylor, C. R. (1981b). Design of the mammalian respiratory system: VIII. Capillaries in skeletal muscles. *Respir. Physiol.* **44**, 129-150.
Hoppeler, H., Lindstedt, S. L., Claassen, H., Taylor, C. R., Mathieu, O. and Weibel, E. R. (1984). Scaling mitochondrial volume in heart to body mass. *Respir. Physiol.* **55**, 131-137.
Howard, C. V. and Reed, M. G. (1998). *Unbiased Stereology: Three Dimensional Measurement in Microscopy*. Oxford: BIOS Scientific Publishers.
Hudlicka, O., Hoppeler, H. and Uhlmann, E. (1987). Relationship between the size of the capillary bed and oxidative capacity in various cat skeletal muscles. *Pflugers Arch.* **410**, 369-375.
Hudlicka, O., Brown, M. and Egginton, S. (1992). Angiogenesis in skeletal and cardiac muscle. *Physiol. Rev.* **72**, 369-417.
Jarman, P. J. (1974). The social organisation of antelope in relation to their ecology. *Behaviour* **48**, 215-267.
Kaijser, L. and Berglund, B. (1992). Myocardial lactate extraction and release at rest and during heavy exercise in healthy men. *Acta Physiol. Scand.* **144**, 39-45.
Kilmer, J. T. and Rodríguez, R. L. (2017). Ordinary least squares regression is indicated for studies of allometry. *J. Evol. Biol.* **30**, 4-12.
Lindstedt, S. L. and Schaeffer, P. J. (2002). Use of allometry in predicting anatomical and physiological parameters of mammals. *Lab. Anim.* **36**, 1-19.
Massie, B. M., Schwartz, G. G., Garcia, J., Wisneski, J. A., Weiner, M. W. and Owens, T. (1994). Myocardial metabolism during increased work states in the porcine left ventricle *in vivo*. *Circ. Res.* **74**, 64-73.
Mathieu-Costello, O. (1993). Comparative aspects of muscle capillary supply. *Annu. Rev. Physiol.* **55**, 503-525.
Mathieu, O., Krauer, R., Hoppeler, H., Gehr, P., Lindstedt, S. L., Alexander, R. M., Taylor, C. R. and Weibel, E. R. (1981). Design of the mammalian respiratory system: VII. Scaling mitochondrial volume in skeletal muscle to body mass. *Respir. Physiol.* **44**, 113-128.
Mayhew, T. M. (1991). The new stereological methods for interpreting functional morphology from slices of cells and organs. *Exp. Physiol.* **76**, 639-665.
Mühlfeld, C., Nyengaard, J. R. and Mayhew, T. M. (2010). A review of state-of-the-art stereology for better quantitative 3D morphology in cardiac research. *Cardiovasc. Pathol.* **19**, 65-82.
Olfert, I. M., Baum, O., Hellsten, Y. and Egginton, S. (2016). Advances and challenges in skeletal muscle angiogenesis. *Am. J. Physiol. Heart Circ. Physiol.* **310**, H326-H336.
Petschow, D., Würdinger, I., Baumann, R., Duhm, J., Braunitzer, G. and Bauer, C. (1977). Causes of high blood O_2 affinity of animals living at high altitude. *J. Appl. Physiol.* **42**, 139-143.
Prothero, J. W. (1979). Heart weight as a function of body weight in mammals. *Growth* **43**, 139-150.
Radloff, F. G. T. and Du Toit, J. T. (2004). Large predators and their prey in a southern African savanna: a predator's size determines its prey size range. *J. Anim. Ecol.* **73**, 410-423.
Schmidt-Nielsen, K. and Pennycuik, P. (1961). Capillary density in mammals in relation to body size and oxygen consumption. *Am. J. Physiol.* **200**, 746-750.

Scott, G. R. (2011). Elevated performance: the unique physiology of birds that fly at high altitudes. *J. Exp. Biol.* **214**, 2455-2462.
Scott, G. R. and Milsom, W. K. (2007). Control of breathing and adaptation to high altitude in the bar-headed goose. *Am. J. Physiol. Regul. Integr. Comp. Physiol.* **293**, R379-R391.
Scott, G. R., Egginton, S., Richards, J. G. and Milsom, W. K. (2009). Evolution of muscle phenotype for extreme high altitude flight in the bar-headed goose. *Proc. R. Soc. Biol. Sci. Ser. B* **276**, 3645-3653.
Scott, G. R., Schulte, P. M., Egginton, S., Scott, A. L. M., Richards, J. G. and Milsom, W. K. (2011). Molecular evolution of cytochrome c oxidase underlies high-altitude adaptation in the bar-headed goose. *Mol. Biol. Evol.* **28**, 351-363.
Scott, G. R., Hawkes, L. A., Frappell, P. B., Butler, P. J., Bishop, C. M. and Milsom, W. K. (2015). How bar-headed geese fly over the Himalayas. *Physiology* **30**, 107-115.
Seymour, R. S. and Blaylock, A. J. (2000). The principle of Laplace and scaling of ventricular wall stress and blood pressure in mammals and birds. *Physiol. Biochem. Zool.* **73**, 389-405.
Smith, R. J. (2009). Use and misuse of the reduced major axis for line-fitting. *Am. J. Phys. Anthropol.* **140**, 476-486.
Snelling, E. P., Taggart, D. A., Maloney, S. K., Farrell, A. P. and Seymour, R. S. (2015a). Biphasic allometry of cardiac growth in the developing kangaroo *Macropus fuliginosus*. *Physiol. Biochem. Zool.* **88**, 216-225.
Snelling, E. P., Taggart, D. A., Maloney, S. K., Farrell, A. P., Leigh, C. M., Waterhouse, L., Williams, R. and Seymour, R. S. (2015b). Scaling of left ventricle cardiomyocyte ultrastructure across development in the kangaroo *Macropus fuliginosus*. *J. Exp. Biol.* **218**, 1767-1776.
Snelling, E. P., Seymour, R. S., Green, J. E. F., Meyer, L. C. R., Fuller, A., Haw, A., Mitchell, D., Farrell, A. P., Costello, M.-A., Izwan, A. et al. (2016). A structure-function analysis of the left ventricle. *J. Appl. Physiol.* **121**, 900-909.
Stahl, W. R. (1965). Organ weights in primates and other mammals. *Science* **150**, 1039-1042.
Stanley, W. C., Recchia, F. A. and Lopaschuk, G. D. (2005). Myocardial substrate metabolism in the normal and failing heart. *Physiol. Rev.* **85**, 1093-1129.
Suarez, R. K. (1996). Upper limits to mass-specific metabolic rates. *Annu. Rev. Physiol.* **58**, 583-605.
van Hall, G. (2010). Lactate kinetics in human tissues at rest and during exercise. *Acta Physiol.* **199**, 499-508.
Vinnakota, K. C. and Bassingthwaighte, J. B. (2004). Myocardial density and composition: a basis for calculating intracellular metabolite concentrations. *Am. J. Physiol. Heart Circ. Physiol.* **286**, H1742-H1749.
Weibel, E. R., Taylor, C. R. and Hoppeler, H. (1991). The concept of symmorphosis: a testable hypothesis of structure-function relationship. *Proc. Natl. Acad. Sci. USA* **88**, 10357-10361.
Weibel, E. R., Taylor, C. R. and Hoppeler, H. (1992). Variations in function and design: testing symmorphosis in the respiratory system. *Respir. Physiol.* **87**, 325-348.
Weibel, E. R., Taylor, C. R. and Bolis, L. (1998). *Principles of Animal Design: The Optimization and Symmorphosis Debate*. Cambridge: Cambridge University Press.
White, C. R. and Seymour, R. S. (2014). The role of gravity in the evolution of mammalian blood pressure. *Evolution* **68**, 901-908.
Woodall, P. F. (1992). Relative heart weights of some African antelope. *J. Zool. (Lond.)* **228**, 666-669.
Zar, J. H. (1998). *Biostatistical Analysis*. New Jersey: Prentice Hall.